Submitted J. Amer. Ceram. Soc.

Spring Constants for Stacks of Curved Leaves of Pyrolytic Boron Nitride

M. L. Kaforey[a], C. W. Deeb[a], & D. H. Matthiesen[a]

Department of Materials Science & Engineering
Case Western Reserve University
Cleveland, OH 44106

Abstract:

Stacks of curved leaves of pyrolytic boron nitride (PBN) were deflected and the force versus deflection data was recorded. From this data, the spring constant for a given spring geometry (radius of curvature of a leaf, width of a leaf, thickness of a leaf, and number of leaves in the stack) was determined. These experiments were performed at room temperature, 500 °C and 1000 °C. However, temperature was not found to affect the spring constant. The measured values were generally within one order of magnitude of predictions made using a previously derived equation for a simply supported cylindrical section with a line force at the center.

---

[a] Member of the American Ceramic Society

Based in part on the thesis submitted by C. W. Deeb for the M.S. degree in Materials Science & Engineering, Case Western Reserve University, Cleveland, OH, 1999.

Supported by Microgravity Science & Applications Division, NASA, under grant number NAG8-1268.

1. Introduction

Ceramic springs composed of stacks of curved pyrolytic boron nitride (PBN) leaves have been used in semiconductor solidification experiments in microgravity[1-4]. The springs were used to accommodate the volume change due to the shrinkage of the semiconductor upon melting. In order to design appropriate springs for use in future experiments, it is necessary to be able to predict the spring constant for a given spring geometry.

PBN is a highly anisotropic material with a hexagonal crystal structure having a *c/a* ratio[5] of approximately 2.64. When produced by chemical vapor deposition, the microstructure generally consists of thin, flat plates with the *c*-axis perpendicular to the substrate surface[6]. Thus, the *c*-axis will be perpendicular to the surface of curved leaves of PBN produced by chemical vapor deposition.

2. Theoretical background and predictions

Consider a curved leaf of PBN cut from a cylinder of radius r with a width w, depth $b = w$, and thickness h as shown in Figure 1. This leaf has an angular leaf span, θ, defined by

$$\theta = 2\arcsin\left(\frac{w}{2r}\right) \tag{1}$$

where w and r are defined above.

A theoretical equation was derived previously to predict the deflection for a simply supported cylindrical section with a line force applied at the center[7]. This equation is

$$d = \frac{Pr}{8E_{eff}I}\left\{-4rw + 2rw\sqrt{4-\frac{w^2}{r^2}} + r^2\theta + \frac{w^2\theta}{2} - r^2\sin\theta\right\} \tag{2}$$

where d is the deflection, P is the applied load, E_{eff} is the effective elastic modulus, and I is the moment of inertia defined by

$$I = \frac{bh^3}{12} \qquad (3)$$

where b and h are defined above.

Considering a stack of leaves, the spring constant, k, of the stack can be predicted as

$$k_p = \frac{P}{dn} = \frac{2E_{eff}bh^3}{3rn\left\{-4rw + 2rw\sqrt{4 - \frac{w^2}{r^2}} + r^2\theta + \frac{w^2\theta}{2} - r^2\sin\theta\right\}} \qquad (4)$$

where n is the number of leaves in the stack.

In order to determine the appropriate elastic modulus for PBN leaf springs, experiments were performed on individual curved leaves of PBN[7]. The effective modulus was found to vary as a function of the angular leaf span, θ, from the pure shear modulus for a flat plate ($\theta = 0$) to a mixed mode modulus for a half cylinder ($\theta = \pi$). For the intermediate cases, the predicted effective modulus, E_{eff}, was found to vary as a function of the angular leaf span according to

$$E_{eff} = E_{FP}\left[1 - \sin\left(\frac{\theta}{2}\right)\right] + E_{HC}\sin\left(\frac{\theta}{2}\right) \qquad (5)$$

where E_{FP} is the modulus for a flat plate[8] (2.60 GPa) and E_{HC} is the effective modulus for a half cylinder[7] (13.41 GPa). Using equations (4) and (5), the behavior of individual PBN leaves were predicted to within 30 % for the majority of cases.

3. Experimental Procedure

The springs were made by cutting PBN Vertical Bridgman crucibles (Advanced Ceramics Co., Cleveland, OH) according to the following procedure. The seedwell and taper were cut from the rest of the crucible, leaving a cylinder of radius, r. The radii for the cylinders used on this work were 64.8 mm (2.55 in), 39.4 mm (1.55 in), and 28.58 mm (1.125 in). The c-axis of the crystallites is perpendicular to the surface to the cylinder. The cylinders were cut into

strips of width, w. The widths of the leaves used in these experiments were 15.2 mm (0.60 in), 12.1 mm (0.475 in), and 8.9 mm (0.35 in). The strips were then cut to give the desired depth, b. In all cases, the depth was cut such that $b = w$.

Springs were thinned to the desired thickness by separating along pyrolytic layers using a razorblade. The thicknesses used in these experiments were nominally 0.25 mm (0.010 in), 0.51 mm (0.020 in), and 0.76 mm (0.030 in). Any spring within ± 0.12 mm (0.005 in) of the nominal thickness was considered acceptable.

The leaves were cleaned with acetone after cutting and then baked out in air in a small box furnace at 500 °C overnight. In general, the leaves were very white after cleaning with rare cases of residual carbon remaining on the surface.

The leaves were stacked in a fused quartz spring chamber with alternating curvature (one concave down and the next concave up). This stacking was repeated until the desired number of leaves, n, was used. The number of leaves used in the spring stacks in these experiments were 10, 20, 30, 40, 75, and 110. Additionally, each successive pair of springs was rotated by 90°. This rotation was done in an effort to reduce the likelihood of "buckling" or sticking of the spring against the spring chamber. A few experiments were performed without this rotation to prove that the spring constant was not affected by this procedure. The data from springs without rotation fell within one standard deviation of the data for springs with rotation[9]. Figure 2 shows a photograph of a typical spring including rotation.

The spring chamber was necessary to keep the springs aligned and upright. The interior of the spring chamber had a square cross-section as did the leaves, but was slightly oversized to allow free motion of the springs during compression. Fused quartz spring chambers were cut to

lengths ranging from 130 mm to 176 mm. Spring chambers were used repeatedly for multiple spring stacks.

The springs were tested in compression using a mechanical testing system (Instron Model 1125, Instron Corp., Canton, MA). An alumina rod was used as a ram to provide rigidity during the tests and compatibility with the high temperature tests. Fused quartz was used as a pedestal for the experiments. Fibrous alumina was used at both the top and the bottom to provide thermal insulation for the high temperature tests. The insulation was kept in place for the room temperature tests for consistency. During the 1000 °C experiments, nitrogen flow through the inlet on the pedestal and then through the chamber was controlled to between 3.5 ± 0.5 L/min. Figure 3 shows a photograph of the furnace opened slightly so that the experimental setup was visible.

For the 500 °C tests, the furnace was ramped to temperature in 20 minutes. For the 1000 °C tests, the furnace was ramped to temperature in 40 minutes. A furnace soak continued until the furnace temperature was maintained in the range of +/- 2 °C of the desired temperature and then the test was started.

The data was recorded directly onto chart paper to obtain continuous data collection. Each cycle consisted of applying a load at 10 mm/min, pausing until steady state was reached, and unloading the sample at 10 mm/min. Each sample was cycled at least 6 times and data was recorded for all cycles. The maximum deflection for each case was determined by the more limiting of the maximum deflection to flatten the leaf or the maximum load of the load cell.

The steady state load, P, and the maximum deflection, d, were measured for each cycle. A value for $k = P / d$ was calculated for each cycle. The first two cycles for each sample were discarded because these cycles sometimes show unusual jaggedness due to slippage of springs

and settling of contact points throughout the system that are not seen in later cycles. The spring constants for remaining cycles were averaged, resulting in one average spring constant, k, for each spring experiment.

4. Results

It was observed visually that in the cases of tall (large n) spring stacks or stacks of leaves having a high degree of curvature, the deflection was not distributed evenly throughout the stack. This observation lead to the hypothesis that the springs were interacting with the spring chamber. That is, one spring or a pair of springs would become wedged in the spring chamber in a position such that it no longer transmitted the load to the springs below it. This interaction with the spring chamber resulted in a variety of features that were seen in the chart recordings at different stages of the cycles including: jaggedness during loading, a load overshoot at the maximum deflection to a value considerably higher than the steady value, and a sharp decrease at the start of unloading.

Figure 4 contains a typical chart recording for one cycle of a spring stack experiment. The loading curve did not increased monotonically in all cases, showing considerable jaggedness in some cases. The general trend however, ignoring jaggedness, was monotonically increasing in all cases. A load overshoot at the maximum deflection occurred in many of the tests. For some of the experiments, it took up to three minutes for the spring to settle to a steady load. The unloading curves for all spring stacks were very similar, with an initial quick unloading and subsequent slow decay to zero load.

In some cases, the curvature during loading was approximately linear as expected for a constant spring constant. However, in other cases, the curvature was continuously increasing in a nearly parabolic fashion. The behavior was closer to linear for flatter springs (smaller θ) and

shorter stacks. The non-linear behavior exhibited by stacks of highly curved springs was believed to be due to the distortion from a perfectly cylindrical section that occurred upon deflection.

Table 1 contains the results of the spring experiments including the average spring constant calculated from a minimum of 4 cycles (after discarding the first 2 cycles). Note that the average spring constants ranged over 2 orders of magnitude from 0.21 (test # 27) to 25.15 N/mm (test # 41).

5. Discussion

For each of the springs tested, a spring constant was predicted using equations (4) and (5). Figure 5 shows a log-log graph of the measured spring constant versus the predicted spring constant. From this graph it can be seen that the measured value was never less than the predicted value. The measured value was generally within one order of magnitude larger than the prediction and always within 1.5 orders of magnitude. Thus, k_P can be used as a lower limit and .5 times k_P can be used as an upper limit for *a priori* predictions of the spring constant for a given geometry. On the log-log graph, there is a fairly constant range of scatter in the data. This indicates a percent error structure.

The residuals (the difference between the natural log of the measured value and the natural log of the predicted value or $(\ln k - \ln k_p)$) were compared as a function of each of the variables. Figure 6 shows the residuals as a function of temperature. The predictions were as accurate at high temperatures as they were at room temperature. There was no significant variation as a function of temperature. In general, elastic moduli vary as a function of temperature, so a dependence on temperature would be expected. However, for the PBN leaves in consideration, more than one elastic modulus is influencing the experiments. Data for the

elastic moduli of PBN as a function of temperature were not available, but some data were found for pyrolytic graphite. Since these materials have similar structures, similar dependence on temperature would be expected. The elastic modulus for a flat plate (E_{FP}) of pyrolytic graphite[10] tested in three-point bending with the pyrolytic layers perpendicular to the compression direction was found to increase slightly (approximately 5 %) as a function of temperature in the range from room temperature to 1000 °C. The other modulus of interest is the modulus parallel to the pyrolytic layers ($E_{//a}$) which contributes to the effective modulus for curved leaves (through the modulus for a half cylinder, E_{HC}). In the range from room temperature to 1000 °C, $E_{//a}$ for pyrolytic graphite[10] was found to decrease by 15 %. Since E_{FP} and $E_{//a}$ both contribute to E_{HC}, and since E_{FP} has a larger impact on E_P than E_{HC} for the angular leaf spans used in these experiments, it is not surprising that the effective modulus did not change much as a function of temperature. Thus, the experimental spring stack experiments that show no effect of temperature are reasonable.

For the variables w, r, and n, the residuals were evenly scattered across the range of the variable. That is, there was no dependence of the residual on these variables. However, for thickness, h, the residuals decreased with increasing thickness as shown in Figure 7. This indicates that the predictions from the theoretical equation are more accurate for springs made from thicker leaves. The thickest leaves (represented by a circle) fall closest to the predicted line as seen in Figure 5.

6. Conclusions

Large springs made of stacks of curved leaves of PBN were fabricated and tested experimentally. For each spring, the steady state load and maximum deflection were measured from the force versus deflection data and a spring constant was calculated. Additionally, a

prediction of the spring constant for each spring was made using an equation based on the deflection equation for a simply supported cylindrical section with a line force applied at the center. The prediction provided a lower bound on the actual spring constant with measured values generally falling within one order of magnitude larger than the prediction.

The measured spring constants were not found to depend on temperature. This was explained due to the variation of the relevant elastic moduli as a function of temperature (E_{FP} increases while $E_{//a}$ decreases). Thus, spring constants measured for particular springs at room temperature will have very similar behavior at high temperatures. This is a particularly useful result for designing springs for crystal growth applications at high temperatures since the design can be tested at room temperature and expected to function the same at the processing temperature.

In semiconductor solidification processing, the most common design failure of a helical graphite spring has been the use of a spring that was too stiff and forced the liquid out of the desired area of the growth system[11]. The current work provides a predictive equation for determining *a priori* the bounds on the spring constant for a spring of a given geometry. Using this equation, springs can be designed to meet the physical constraints of a system so that they will not exceed the maximum acceptable force applied to the liquid.

The deflection and spring constant prediction equations used in this work could be applied to other materials systems. They are appropriate for curved leaves cut from cylinders of any material. The prediction of the effective modulus as a function of angular leaf span would be expected to apply to any layered structure in which the layers were configured in the same way, that is, in any material in which the layers are perpendicular to the circumference of the cylinder.

7. References

1. M. L. Kaforey, J. M. Bly and D. H. Matthiesen, "Void Formation in Gallium Arsenide Crystals Grown in Microgravity." J. Cryst. Growth **174**, 112-119 (1997).
2. D.H. Matthiesen and J.A. Majewski, "The Study of Dopant Segregation Behavior During the Growth of GaAs In Microgravity"; pp. 232-262 in NASA Joint Launch+1 Year Science Review, Vol. 1. NASA Conference Publication 3272, May 1994.
3. D.H. Matthiesen, M.L. Kaforey, and J.M. Bly, "Experiment XIII. The Study of Dopant Segregation Behavior During the Growth of GaAs in Microgravity on USML-2"; pp. 293-335 in Second United States Microgravity Laboratory: One Year Report, Vol. 1. NASA TM-1998-208697, August 1998.
4. J.M. Bly, M.L. Kaforey, D.H. Matthiesen, and A. Chait, "Interface Shape and Growth Rate Analysis of Se/GaAs Bulk Crystals Grown in the NASA Crystal Growth Furnace (CGF)," J. Cryst. Growth **174**, 220-225 (1997).
5. R.S. Pease, "An X-ray Study of Boron Nitride," Acta Cryst. **5**, 356-361 (1952).
6. L. Duclaux, B. Nysten, J-P. Issi, and A.W. Moore, "Structure and Low-temperature Thermal Conductivity of Pyrolytic Boron Nitride," Phys. Rev. B **46** [6] 3362-3367 (August 1992).
7. M. L. Kaforey, C. W. Deeb, and D. H. Matthiesen, "Effective Elastic Modulus as a Function of Angular Leaf Span for Curved Leaves of Pyrolytic Boron Nitride," submitted to J. Am. Ceram. Soc. (1999).
8. M. L. Kaforey, C. W. Deeb, D. H. Matthiesen, and D. J. Roth, "Elastic Moduli of Pyrolytic Boron Nitride Measured Using 3-Point Bending and Ultrasonic Testing," submitted to J. Am. Ceram. Soc. (1999).

9. C. W. Deeb, "Mechanical Characterization of Pyrolytic Boron Nitride (PBN) Leaf Springs," M.S. Thesis, Materials Science & Engineering (Case Western Reserve University, Cleveland, OH, 1999).

10. M.B. Dowell, Advanced Ceramics, Cleveland, OH, private communication (1992).

11. K. Kinoshita and T. Yamada, "$Pb_{1-x}Sn_xTe$ crystal growth in space," J. Cryst. Growth 147 (1995) 91.

12. K. Kinoshita and T. Yamada, "Spherical crystals of $Pb_{1-x}Sn_xTe$ grown in microgravity," J. Cryst. Growth 165 (1996) 75.

8. Figure Captions

Figure 1. Schematic showing (a) end view of PBN cylinder of radius, r, and cylindrical section of width, w, and (b) individual leaf of thickness, h, and depth, b, with force applied at centerline.

Figure 2. Fused quartz spring chamber containing a stack of spring leaves with r = 64.8 mm (2.55 in), w = 15.2 mm (0.60 in), h = 0.76 mm (0.03 in), and n = 110 leaves prior to the first compression cycle.

Figure 3. Photograph of a spring loaded in the mechanical testing system with the furnace opened slightly.

Figure 4. Typical chart data for a spring stack with deflection, d = 7.5 mm and steady load, P = 4.76 N.

Figure 5. Log-log graph of average spring constant versus predicted spring constant for spring stack experiments.

Figure 6. Graph of residuals ($\ln k_m - \ln k_p$) versus temperature for spring stack experiments indicating that there was no significant variation as a function of temperature.

Figure 7. Graph of residuals ($\ln k_m - \ln k_p$) versus thickness for spring stack experiments indicating a closer agreement with predicted values for thicker leaves.

Table 1. Experimental results of spring stack experiments.

Test #	Width, w (mm)	Radius, r (mm)	Thickness, h (mm)	Number, n	Temperature (°C)	Average spring constant, k (N/mm)
1	15.2	64.8	0.76	40	1000	2.47
2	12.1	39.4	0.51	75	500	0.86
3	12.1	39.4	0.25	75	500	0.29
4	15.2	64.8	0.25	110	23	0.14
5	12.1	39.4	0.76	75	500	1.45
6	12.1	39.4	0.51	110	500	0.77
7	8.9	64.8	0.25	40	23	1.04
8	12.1	28.6	0.51	75	500	2.19
9	15.2	28.6	0.76	75	1000	6.02
10	15.2	28.6	0.76	40	23	5.02
11	12.1	39.4	0.51	75	1000	0.92
12	15.2	28.6	0.25	40	1000	0.44
13	8.9	28.6	0.25	40	23	1.03
14	12.1	39.4	0.51	75	23	0.88
15	8.9	64.8	0.25	40	1000	1.39
16	12.1	39.4	0.51	40	500	1.05
17	15.2	64.8	0.25	40	23	0.51
18	15.2	39.4	0.51	75	500	2.01
19	8.9	28.6	0.76	110	23	2.49
20	8.9	64.8	0.76	110	1000	1.81
21	12.1	64.8	0.51	75	500	1.19
22	12.1	39.4	0.51	75	500	0.69
23	15.2	28.6	0.25	110	23	0.28
24	8.9	28.6	0.76	40	1000	5.26
25	8.9	64.8	0.76	40	23	2.38
26	12.1	39.4	0.51	75	500	0.69
27	15.2	64.8	0.25	110	1000	0.21
28	12.1	39.4	0.51	75	500	0.55
29	15.2	64.8	0.76	110	23	1.00
30	8.9	28.6	0.25	110	1000	0.59
31	8.9	39.4	0.51	75	500	2.03
32	8.9	64.8	0.25	110	23	0.24
33	12.1	39.4	0.51	75	500	1.01
34	15.2	64.8	0.76	10	23	7.78
35	8.9	28.6	0.25	30	23	2.14
36	12.1	39.4	0.51	20	23	1.58
37	15.2	28.6	0.25	10	23	1.31
38	15.2	28.6	0.76	30	23	5.18
39	12.1	39.4	0.51	20	23	1.19
40	8.9	64.8	0.76	30	23	5.79

41	8.9	28.6	0.76	10	23	25.15
42	12.1	39.4	0.51	20	23	1.74
43	15.2	64.8	0.25	30	23	0.56
44	8.9	64.8	0.25	10	23	4.47
45	12.1	39.4	0.51	20	500	2.44
46	8.9	28.6	0.25	10	1000	3.95
47	12.1	28.6	0.51	20	500	3.78
48	15.2	28.6	0.76	10	1000	9.13
49	12.1	39.4	0.76	20	500	6.41
50	15.2	28.6	0.25	30	1000	0.54
51	12.1	39.4	0.51	20	1000	1.45
52	8.9	64.8	0.25	30	1000	3.20
53	12.1	39.4	0.25	20	500	0.54
54	12.1	39.4	0.51	20	500	1.61
55	15.2	64.8	0.25	10	1000	4.76
56	15.2	39.4	0.51	20	500	2.01
57	8.9	39.4	0.51	20	500	5.26
58	12.1	64.8	0.51	20	500	3.73
59	8.9	64.8	0.76	10	1000	10.96
60	8.9	28.6	0.76	30	1000	4.48
61	12.1	39.4	0.51	10	500	2.89
62	15.2	64.8	0.76	30	1000	2.30
63	12.1	39.4	0.51	30	500	1.01
64	12.1	39.4	0.51	20	500	1.19

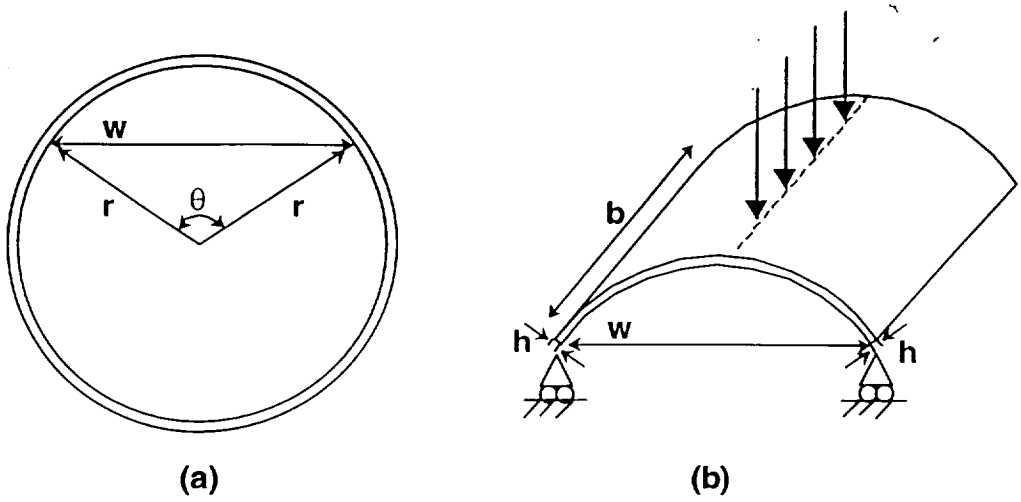

Figure 1. Schematic showing (a) end view of PBN cylinder of radius, *r*, and cylindrical section of width, *w*, and (b) individual leaf of thickness, *h*, and depth, *b*, with force applied at centerline.

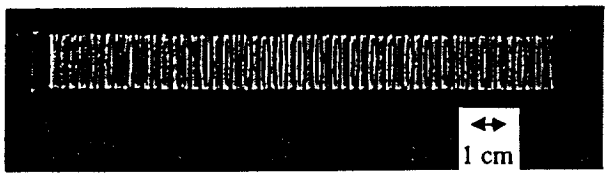

Figure 2. Fused quartz spring chamber containing a stack of spring leaves with r = 64.8 mm (2.55 in), w = 15.2 mm (0.60 in), h = 0.76 mm (0.03 in), and n = 110 leaves prior to the first compression cycle.

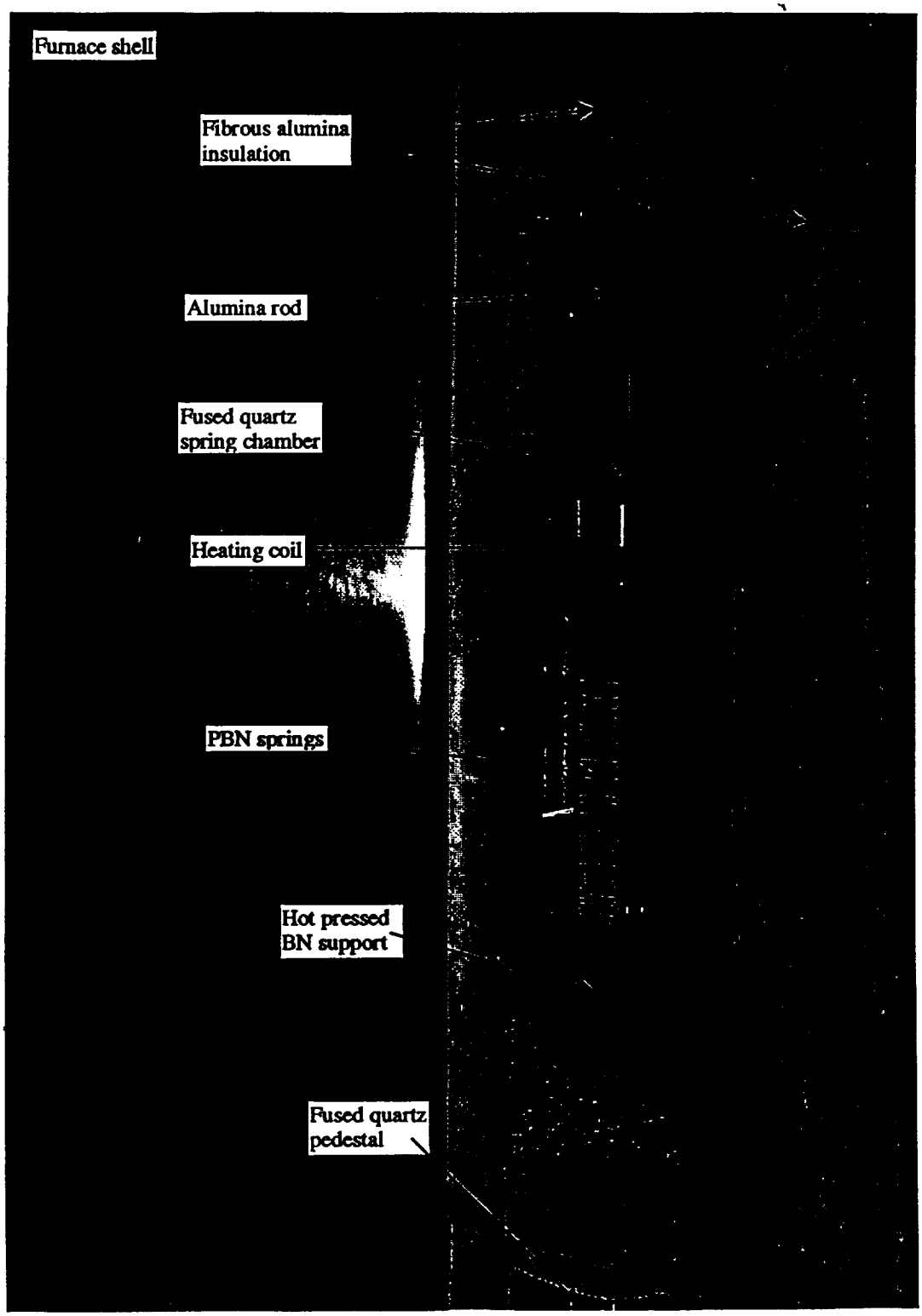

Figure 3. Photograph of a spring loaded in the mechanical testing system with the furnace opened slightly.

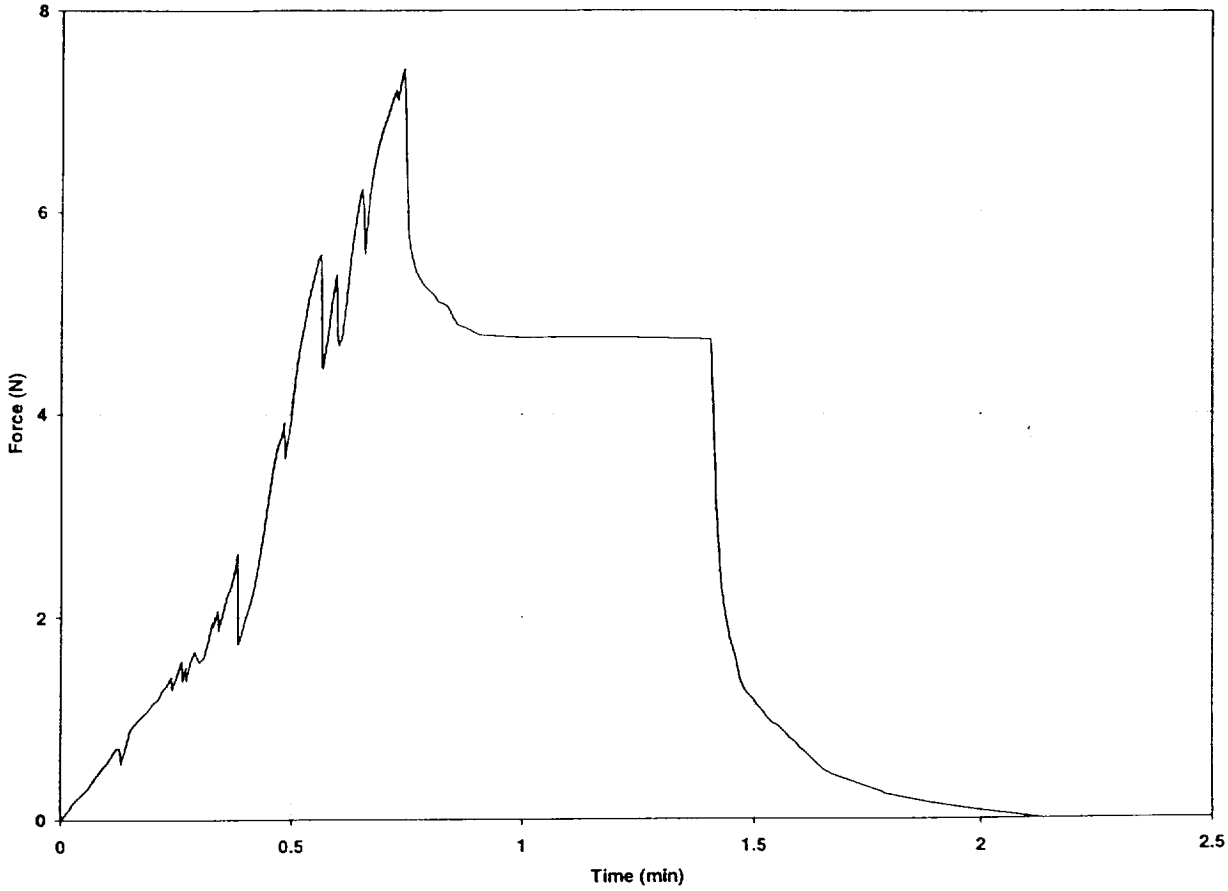

Figure 4. Typical chart data for a spring stack with deflection, d = 7.5 mm and steady load, P = 4.76 N.

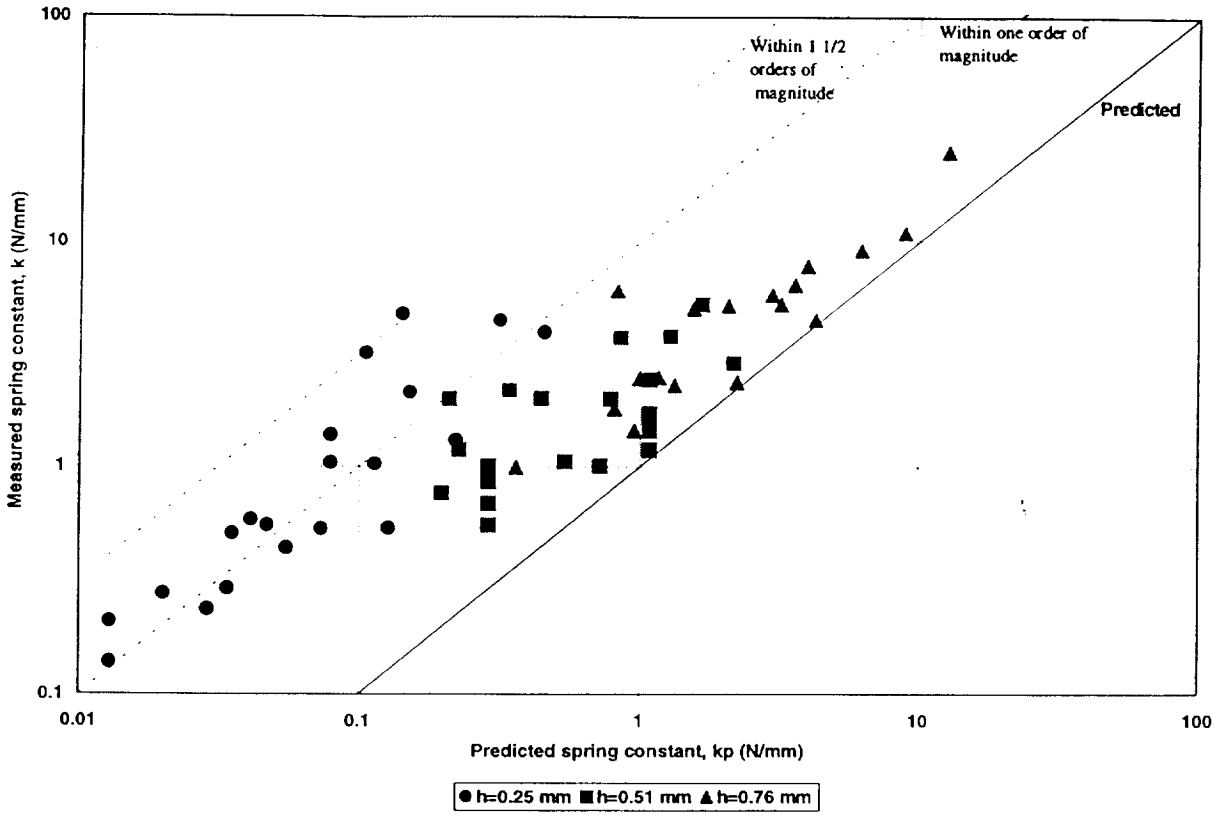

Figure 5. Log-log graph of average spring constant versus predicted spring constant for spring stack experiments.

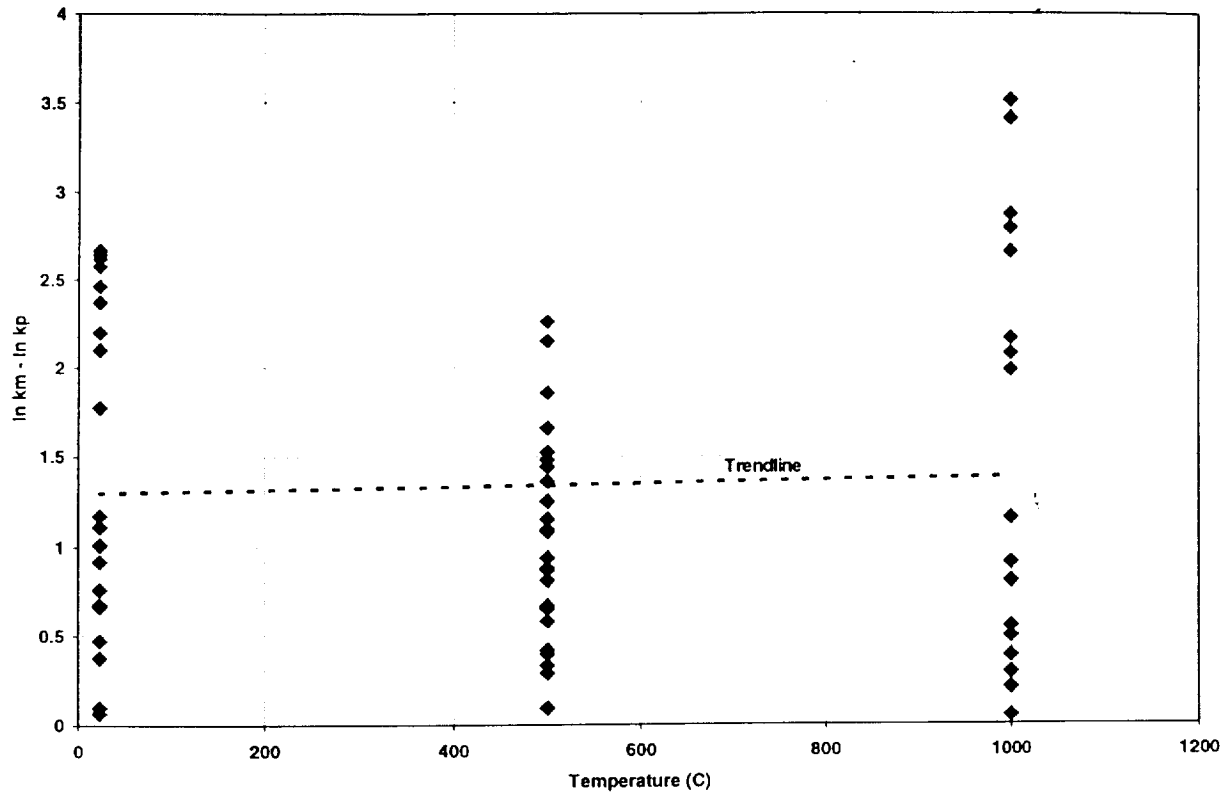

Figure 6. Graph of residuals ($\ln k_m - \ln k_p$) versus temperature for spring stack experiments indicating that there was no significant variation as a function of temperature.

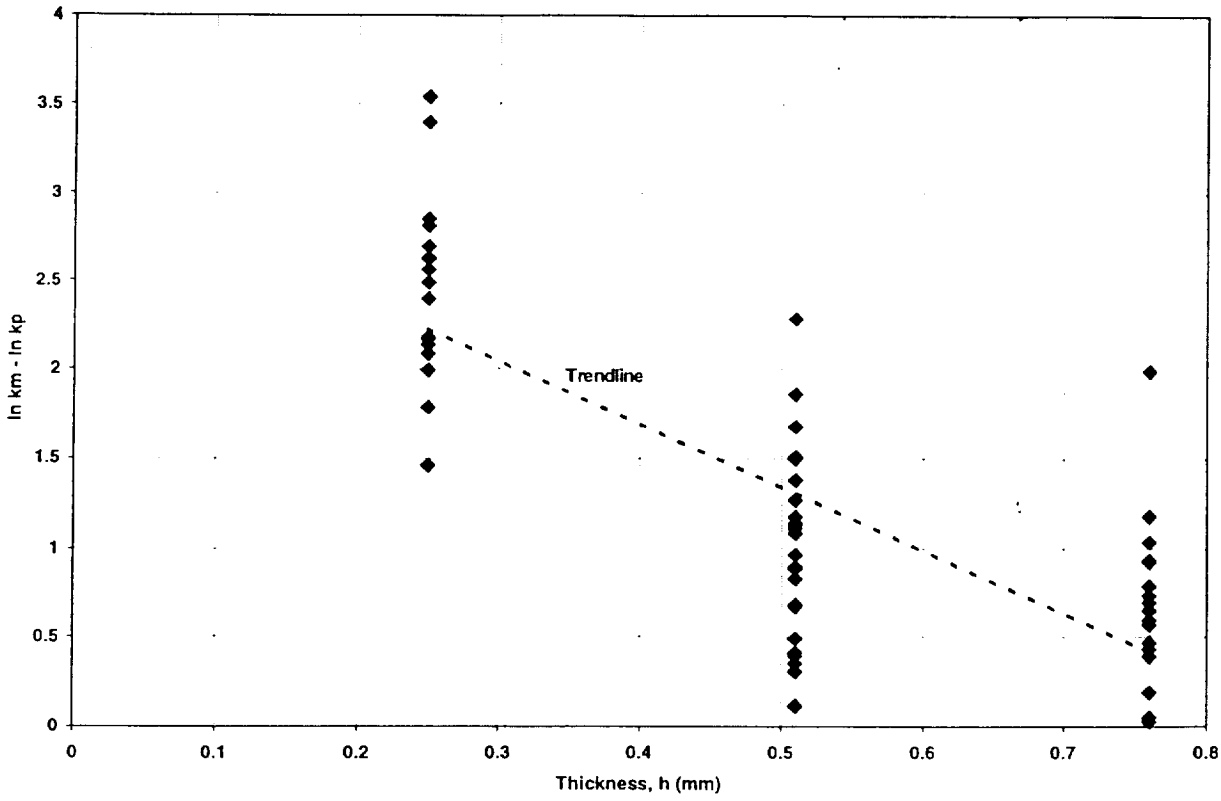

Figure 7. Graph of residuals (ln k_m – ln k_p) versus thickness for spring stack experiments indicating a closer agreement with predicted values for thicker leaves.